

Variations in wetland conditions within the Fitzroy Basin, north-eastern Australia: a palaeoecological approach

Johanna M. Hanson^{ID A,C,D}, Maria L. VanderGragt^B, Kevin J. Welsh^A and Patrick T. Moss^A

^ASchool of Earth and Environmental Sciences, University of Queensland, 280-284 Sir Fred Schonell Drive, St Lucia, Brisbane, Qld 4067, Australia.

^BDepartment of Environment and Science, Queensland Government, 41 Boggo Road, Dutton Park, Brisbane, Qld 4102, Australia.

^CSchool of Earth and Environment, University of Canterbury, 20 Kirkwood Avenue, Upper Riccarton, Christchurch 8041, New Zealand.

^DCorresponding author. Email: johanna.hanson@pg.canterbury.ac.nz

Abstract. The North-east Australian Coastal Catchments (NACC) are host to nationally significant wetland complexes, many of which, are ecologically connected to the Great Barrier Reef World Heritage area. However, these wetlands are subject to ongoing and increasing pressure from human activities such as the intensification of land use. Current wetland condition is monitored across the NACC, being assessed against a pre-development static baseline, which includes the use of Regional Ecosystem mapping of remnant and pre-clearing vegetation to provide a broadscale present-day biotic reference. Two sediment cores from wetlands within the Fitzroy Basin were analysed to establish a history of wetland variability and to identify the potential influence of climate and land-use changes over the past ~1000 years. Our results have provided long-term environmental reconstructions, showing wetland histories influenced by natural climate variability (El Niño–Southern Oscillation, the Little Ice Age), and environmental changes associated with European land-use intensification. This study is the first of its kind for wetlands located within the Fitzroy Basin.

Keywords: environmental impact, Great Barrier Reef catchment, hydrology, millennial climate drivers, land-use intensification, wetland variability.

Received 10 March 2021, accepted 26 July 2021, published online 14 September 2021

Introduction

Globally, wetlands are under pressure from climate change and human land-use intensification (Dudgeon *et al.* 2006; Gangloff *et al.* 2016; Finlayson *et al.* 2017; Reid *et al.* 2019). Such pressures on wetlands include hydrological modification (Schneider *et al.* 2017), increased runoff and sedimentation rates (Ogden 2000), increased nutrients and pollutants (Gell *et al.* 2009), the introduction of exotic species (Finlayson and Rea 1999) and extreme climatic conditions (Pasut *et al.* 2021). These, and other pressures, are also affecting wetlands situated in catchments of the north-eastern Australian coast. Since European arrival, the North-east Australian Coastal Catchments (NACC) have undergone significant land-use changes, for example, agriculture, forestry, mining and urban townships (Gilbert 2000; Australian Government: Great Barrier Reef Marine Park Authority 2001; Lewis *et al.* 2021). Recognising the importance of wetland ecosystem intrinsic values, and the services they provide, presents a significant foundation for understanding the conditions of freshwater wetlands located within the NACC, which is an objective of the Australian and Queensland Governments as part

of the Reef 2050 Long-term Sustainability Plan (Commonwealth of Australia 2015; Australian Government and Queensland Government 2016; State of Queensland 2018). The condition of wetlands located in floodplain aggregations is monitored across the NACC as part of the Paddock to Reef Wetland Condition Monitoring Program (Australian Government and Queensland Government 2016; State of Queensland 2018; Waterhouse *et al.* 2018), to inform overall management and restoration directions and programs for improvement of wetland condition. Rapid-assessment indicators are used (Australian Government and Queensland Government 2016; Waterhouse *et al.* 2018), including measures of the extent and integrity of native vegetation pre-clearing Regional Ecosystems (i.e. native vegetation associated with specific geology, soil and geomorphic processes within prescribed bioregions) as mapped by the Queensland Herbarium. Pre-cleared vegetation or Regional Ecosystems are defined as ‘the vegetation or Regional Ecosystem present before clearing’ (i.e. ‘pre-1750 CE’ or ‘pre-European’; Neldner *et al.* 2019). The status of Regional Ecosystems is considered an important indicator of catchment modification and wetland

biophysical integrity (Queensland Government 2014; State of Queensland 2018).

Palaeoecological research shows that wetlands are dynamic systems with considerable variability over very long time periods and can provide important insights into pre-European conditions as well as anthropogenic impacts (e.g. Gell and Reid 2014; Gell *et al.* 2016; Wingard *et al.* 2017). Palaeoecological studies of NACC wetlands are limited; however, Tibby *et al.* (2019) provided two palaeolimnological records from two tropical floodplain wetlands within the Burdekin Catchment, Queensland, Australia. Natural variability and wetland stressors were examined, with minor ecological change due to land clearing for grazing; however, hydrological modification caused a shift in diatom assemblage and increased invasive aquatic taxa. These findings were correlated with modern diatom samples from wetlands situated around the Burdekin Catchment, and it has been suggested that this shift from historical conditions (seen at Labatt Lagoon) may be widespread around the lower Burdekin River area. However, more site-specific research would be required to ascertain this. Thus, there is need for greater knowledge of historical wetland states and transitions to contextualise current monitoring baselines and, ultimately, support management decision-making.

To this end, a study of sediment cores taken from two wetlands in the Fitzroy Basin (within the Brigalow Belt bioregion) was undertaken to determine the degree to which the pre-European vegetation baselines (Regional Ecosystem classification scheme), which are used to assess wetlands, reflect long-term conditions. This study will also identify wetland variability due to changing environmental conditions and any alterations in land use.

Fitzroy Basin

The Fitzroy Basin, located in central Queensland, covers an area of 142 665 km² and is the largest river catchment flowing into the Great Barrier Reef lagoon on the eastern coast of Australia. This basin is made up of seven subcatchments, including the Fitzroy River catchment and the Dawson River catchment (see Fig. 1; State of Queensland 2018). Nationally important aggregations of remnant wetlands are located in these catchments (The State of Queensland 2020; Department of Agriculture, Water and the Environment, n.d.).

Within the NACC, the Fitzroy Basin has seen the most widespread and rapid land-use intensification. Indigenous peoples have inhabited and managed the land in this area for at least the past ~40 000 years before present (Walsh 1999), with European occupation influencing the landscape from the 1840s CE (Seabrook *et al.* 2006). Seabrook *et al.* (2006) determined four stages of changing land use in the region. Initially, large pastoral runs were established between 1840 CE and 1880 CE, followed by a closer settlement scheme (between 1880 CE and 1940 CE) that included mixed farming and smaller grazing leases (which required land improvement, e.g. ring-barking). Between 1940 CE and 1990 CE, reductions in farm size occurred, which were followed by the largest land development scheme (Brigalow Development Scheme) ever undertaken in Australia. This continued until the late 1990s CE, resulting in one of the most rapid landscape transformations in Australia. From the 1990s CE to 2006 CE, there was a shift to more sustainable development where attitudes about land clearing (and the environmental impact caused) and climate change proceeded to change policies about managing the environment (e.g. *The Land Act* 1994; *Vegetation Management Act* 1999).

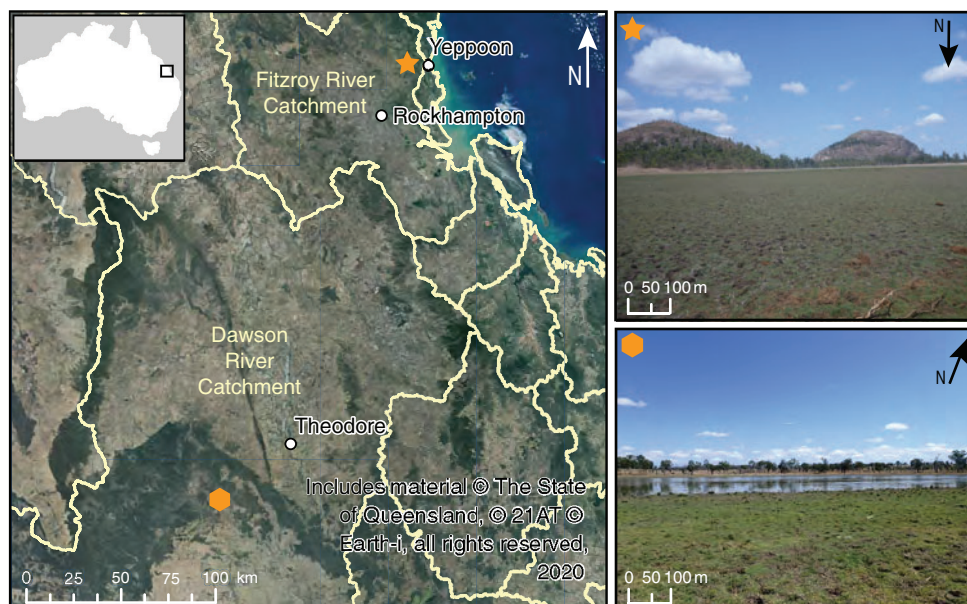


Fig. 1. Map of Australia highlighting central south-eastern Queensland, with satellite imagery showing drainage sub-basins of major river systems in central south-eastern Queensland (courtesy of Terri Sutcliffe). The star indicates Lake Mary North (photograph taken by Patrick Moss, September 2018) and the hexagon represents the location of Tualka (photograph taken by Maria VanderGragt, September 2018).

Study sites

Lake Mary North

Lake Mary North (523.05 ha; wetland mapping V5; [Department of Environment and Science Queensland 2019](#)) is located in the Hedlow wetland aggregation within the Fitzroy River subcatchment ([Fig. 1](#)). It is a floodplain palustrine wetland with a water regime driven primarily by precipitation and evaporation. This wetland is covered by water 40–60% of the time ([The State of Queensland 2020](#)). Lake Mary North is located in the subtropics and is dominated by hot, humid summers ([Köppen 1931](#); [Bureau of Meteorology 2006](#)). Lake Mary North lies on Quaternary alluvium, eroded from Devonian/Carboniferous metamorphic basement rocks ([Willmott *et al.* 1986](#)).

Lake Mary North has a catchment area of 24 210 ha, of which 55% is remnant vegetation ([Queensland Herbarium 2019](#)). Lake Mary North is classified as part of Regional Ecosystem (RE) 8.3.4, which is recorded as a coastal and subcoastal freshwater floodplain wetland with permanent or semi-permanent water with aquatic macrophytes ([Queensland Herbarium 2019](#); K. Glanville, Queensland Herbarium, pers. comm.). On the basis of field observations, present-day vegetation is dominated by pasture grasses during dry periods and populations of aquatic macrophytes during wet periods.

Tualka

The Tualka wetland (77.81 ha; wetland mapping V5; [Department of Environment and Science Queensland 2019](#)) is a floodplain lake on Tualka Creek, located within the Palm Tree Robinson Creek aggregation in the Dawson River subcatchment ([Fig. 1](#); [Queensland Herbarium 2019](#)). The water regime of this lake is influenced by creek flooding and potentially intermittent ground water connectivity and is covered by water 80–100% of the time ([Department of Science, Information Technology and Innovation 2015](#); [The State of Queensland 2020](#)). Tualka is situated in the subtropics, and is dominated by hot, dry summers and cold winters ([Köppen 1931](#); [Bureau of Meteorology 2006](#)). Underlying and surrounding Tualka are the Hutton Sandstone and Boxvale Sandstone, which are both aquifers in the Surat Basin ([Habermehl and Lau 1997](#)).

Tualka has a catchment area of 58 855 ha, 87% of which consists of remnant native vegetation in state forests and national parks ([Queensland Herbarium 2019](#)). This wetland is classified as part of RE 11.3.27g, which proposes an open body of water which may or may not have aquatic macrophytes and has fringing eucalypt woodland (*Eucalyptus coolabah*, *E. populnea* and *Eremophila mitchellii*) and sedgeland ([Queensland Herbarium 2019](#)). Presently, the surrounding landscape is used for grazing purposes ([The State of Queensland 2020](#)).

Materials and methods

Two clay cores (LMN1, 46 cm; TUA1, 45 cm) were extracted via Russian d-section from Lake Mary North (23°06.451'S, 150°35.258'E) and Tualka (25°12.910'S, 149°41.960'E) respectively, in September 2018 ([Fig. 1](#)). These cores underwent sedimentological, geochemical and palaeoecological analyses to determine past wetland variability and to examine the effects of climatic variation and human activities, which may have affected the wetlands and surrounding landscape.

Chronology and sedimentology

Bulk sediment samples from the base of each core (45–46 cm for LMN1 and 43.5–45 cm for TUA1) were sent for radiocarbon dating to Beta Analytic, to obtain basal ages and to constrain the palaeoenvironmental records. A further two samples from LMN1 were taken at 30 and 20 cm and one from TUA1 at 20 cm, which were prepared using [Moss \(2013\)](#) modified version of pollen preparation, for the pollen concentrate to be radiocarbon dated. With bulk sediment analysis, there may be a wider error range than with pollen samples. Using OxCal (ver. 4.4, [Bronk Ramsey 1995, 2008, 2009](#), see <https://c14.arch.ox.ac.uk/oxcal/OxCal.html>), the returned ages were calibrated to the southern hemisphere using the SHCal20 calibration curve, with dates past 1950 CE, calibrated using the post-bomb atmospheric southern hemisphere 1–2 curve ([Hua *et al.* 2013](#); [Hogg *et al.* 2020](#)). After which, Bayesian modelling was used to create age-depth models using the rbacon (ver. 2.5.0) package in RStudio ([Blaauw and Christen 2011](#); R Foundation for Statistical Computing, Vienna, Austria, see <https://www.R-project.org/>; RStudio, PBC, Boston, MA, USA, see <http://www.rstudio.com/>). Both LMN1 and TUA1 were classified using an adapted version of the Troels-Smith peat classification ([Troels-Smith 1955](#); [Kershaw 1997](#)) every 5 cm, to determine changes in visual and physical characteristics along the cores.

Total organic carbon and carbon to nitrogen analyses

Both cores were subsampled every 5 cm for total organic carbon (TOC) and carbon to nitrogen (C:N) ratios, following [Meyers and Teranes \(2001\)](#) method. These samples were dried in an oven for 29 h at 40°C and then crushed into homogenous powder using an agate mortar and pestle. Individual pills were created by measuring 0.1 g of sample into tin foil boats, which were then pressed into pills and weighed again to provide accurate measurements. The samples were analysed using an Elementar MACRO cube at The University of Queensland. To ensure quality assurance and control, blanks were placed at the beginning, end and after every five samples, whereas phenylalanine standards were run at the beginning and end of each core to limit samples with high carbon concentration causing a carry-on carbon effect.

X-ray fluorescence

Using an Olympus Innov-X Handheld X-ray Fluorescence (XRF) Spectrometer (as part of a GEOTEK Multi-Sensor Core Logger at The University of Queensland), both cores were scanned to provide chemical trends for major inorganic elements. XRF is a non-destructive technique to determine trends in elemental composition. This instrument has two calibration modes: (1) soil mode and (2) geochemistry mode. Soil mode produces a more reliable record with 'heavier' elements (e.g. most transition metals and redox sensitive elements, such as iron (Fe) and manganese (Mn)), and geochemistry mode records a lower error rate with 'lighter' elements (e.g. silicon (Si) and aluminium (Al)). A stainless-steel standardisation coin was used to calibrate the XRF spectrometer, before reporting values and errors in milligrams per kilograms (mg/kg). Both cores were analysed at 1 cm intervals with a dwell time of 30 s. Variations in moisture content can attenuate the intensity of light elements

such as Si and Al (Tjallingii *et al.* 2007) and high organic contents can affect the reliability of trace elements (e.g. copper (Cu), nickel (Ni), scandium (Sc)), although titanium (Ti) and Fe are generally thought to be reliable even in highly organic-rich cores (Longman *et al.* 2019). Therefore, even though results are reported in mg/kg, we only consider trends in immobile elements (e.g. zircon (Zr), Ti, Si, Al) as proxies for terrigenous sediment input (as opposed to organic matter; Olsen *et al.* 2010; Kylander *et al.* 2011; Evans *et al.* 2019) in the cores rather than absolute values.

Palaeoecology

Palynological and micro-charcoal analyses were conducted at 5 cm intervals along the cores. These samples were processed by utilising an adapted version (Moss 2013) of van der Kaars (1991) method for pollen extraction from marine sediments. Samples were heated in sodium hexametaphosphate to deflocculate clays, which were then sieved to remove particles greater than 180 µm. Heavy liquid separation (sodium polytungstate; specific gravity 1.9) was then used to isolate the organic fraction from the minerogenic fraction. Samples then underwent acetolysis to dissolve excess cellulose for easier identification and were mounted on slides in glycerol. At least 300 dryland pollen grains (e.g. rainforest, sclerophyll arboreal and herbaceous taxa and pteridophytes) and 200 micro-charcoal particles were identified and counted as per Walter and Willy (2004). A tablet of known concentration of exotic *Lycopodium clavatum* (9666 grains per tablet) was added to each sample at the beginning of preparation to determine pollen and micro-charcoal concentrations (spike concentration method; Wang *et al.* 1999). Because only a small amount of sample is counted, this method suggests how much pollen/micro-charcoal there should be in the initial 1 cm³ sample. This entails dividing the concentration of grains in an exotic *Lycopodium* tablet by the amount of *Lycopodium clavatum* counted and multiplying it by the amount of pollen/micro-charcoal. Using Tilia (ver. 2.6.1, see <https://www.tiliait.com/download/>) data were graphed and classified into biostratigraphic zones by Constrained Incremental Sum of Squares (CONISS) (Grimm 1987).

Results

Chronology and sedimentology

Lake Mary North (LMN1)

As shown in Table 1, LMN1 returned a basal age of 1096–1217 CE at 45 cm. At 30 cm, the age returned was 1876–1945

CE and at 20 cm the returned age was 2003–2007 CE. Rbacon was used to produce an age–depth model using Bayesian modelling and radiocarbon dates. However, the radiocarbon age at 20 cm could not be made to fit the Bayesian model, potentially indicating contamination from younger carbon (Fig. 2). Sediments at Lake Mary North contained substantial modern root mass at the top of the core. An additional tie point for the chronology at Lake Mary North is the observation of introduced vegetation indicative of European occupation (*Plantago lanceolata*) at 15 cm, which is known to have occurred in the 1840s CE in Rockhampton (Seabrook *et al.* 2006). Therefore, the youngest radiocarbon age was rejected and not used in the rbacon age–depth model.

LMN1 is a 46 cm clay sediment core that increases in organic content towards the top of the core (see Supplementary material Table S1). The top 10 cm contains modern root mass and fibrous herb detritus with little clay content. Herbs and fine detritus are common throughout the core and from 46 to 15 cm, iron oxide staining is present. Most of the core is 10YR 2/1 Black; however, between 25–20 cm and between 15–10 cm there is a slight change to 10YR 3/1 Very dark grey. From 10 to 5 cm there is modern root detritus and sediment, while the top 5 cm of the core is modern root mass (top 10 cm is coloured 10YR 6/3 Pale brown).

Tuaka (TUA1)

TUA1 returned a basal age of 1142–1230 CE at 44 cm and 1955–1956 CE at 20 cm (Table 1).

TUA1 is a 45 cm clay core with very slight textural and colour changes, with iron oxide staining throughout the core (see Supplementary material Table S2). At the base of TUA1, woody and herb detritus are present. From 45 to 15 cm and from 10 to 5 cm, macro-charcoal is visible. At 30 cm, there is a shift from 10YR 4/1 Dark grey to 10YR 4/2 Dark greyish brown.

Total organic carbon and carbon to nitrogen analyses

Lake Mary North (LMN1)

For the majority of the Lake Mary North record, TOC values show an increasing trend (Fig. 3). TOC percentages begin low until 30 cm, before peaking at 15 cm, and ending on slightly decreased percentages. The C:N values follow a similar trend; however, they peak earlier (25 cm) and end on slightly increased values.

Tuaka (TUA1)

TUA1 has very low organic matter, with TOC values ranging between 0.83 and 1.28% (Fig. 4). TOC shows a general

Table 1. Returned ages from Beta Analytic, which were calibrated in OxCal (Bronk Ramsey 1995, 2008, 2009) using SHCal20 calibration curve (Hogg *et al.* 2020) and the post-bomb atmospheric southern hemisphere 1–2 curve (Hua *et al.* 2013)

From these ages, age–depth models were determined using the rbacon package on RStudio (Blaauw and Christen 2011; R Foundation for Statistical Computing, see <https://www.R-project.org/>; RStudio, see <http://www.rstudio.com/>)

Depth (cm)	Site name	Dated material	Conventional radiocarbon age	Error	Oxcal calibrated age (CE)
20	LMN1	Pollen extract	–57	4	2003–2007
30	LMN1	Pollen extract	70	30	1876–1945
45	LMN1	Bulk sediment	940	30	1096–1217
20	TUA1	Pollen extract	–35	2	1955–1956
44	TUA1	Bulk sediment	910	30	1142–1230

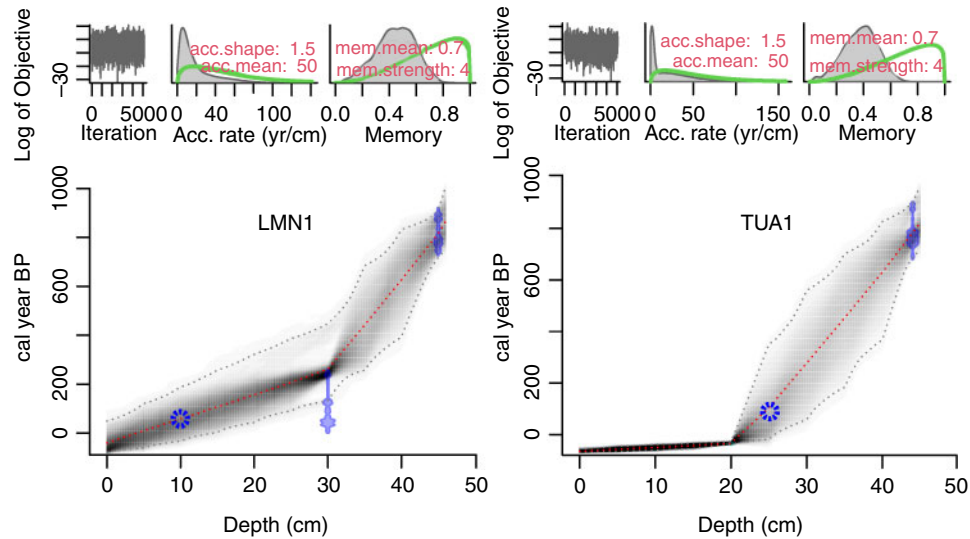


Fig. 2. Age–depth models created using rbacon on RStudio (Blaauw and Christen 2011; R Foundation for Statistical Computing, see <https://www.R-project.org/>; RStudio, see <http://www.rstudio.com/>), with exotic pollen taxa represented by the blue circle.

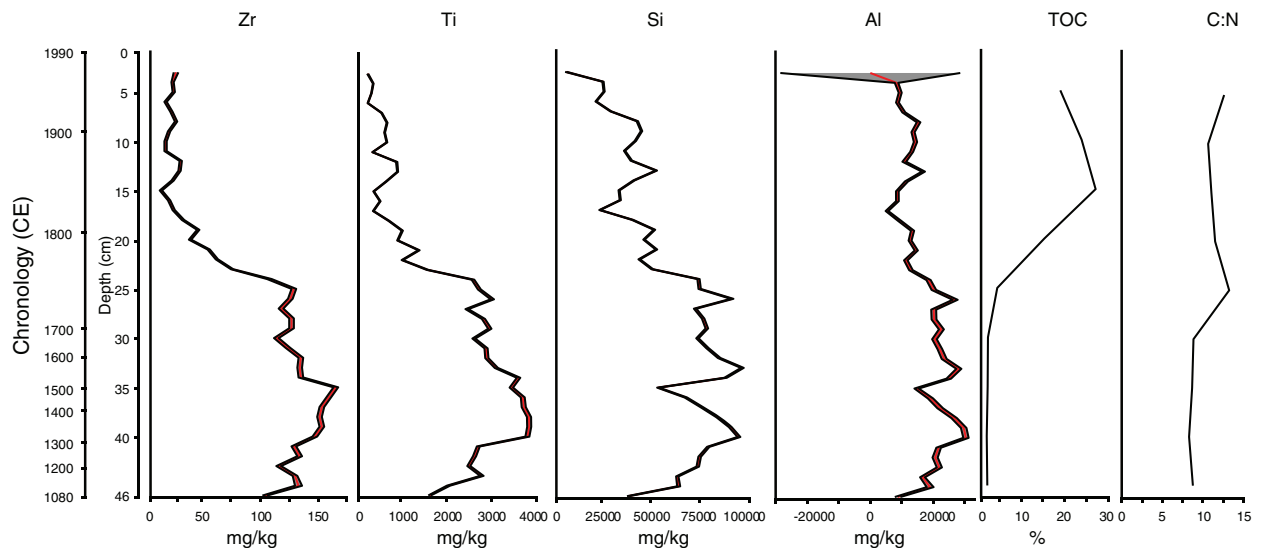


Fig. 3. Lake Mary North diagram showing XRF elements, total organic carbon and carbon to nitrogen ratio. The red line in the XRF is the recorded element in mg/kg, with the black lines on either side representing the measured error rate.

increasing trend, peaking at 30 cm, before slightly decreasing and reaching a plateau $\sim 1\%$ for the rest of the record. The C:N values remain ~ 12 for the entirety of the record, with minimal change.

X-ray fluorescence

Lake Mary North (LMN1)

From the base of the core to 40 cm, all elements show an increasing trend (Fig. 3). Whereas Zr continues to peak at 35 cm, Ti, Si and Al all decline to varying degrees before returning to elevated levels. At 25 cm, all elements show a decreasing trend, with Zr showing the greatest decrease and Al the smallest. At 15 cm, Ti, Si and Al show very low values before slightly

increasing and then returning to lowered values at the top of the core. However, Zr shows an increasing trend from 15 cm to the top of the record.

Tuaka (TUA1)

The base of Tuaka shows high values of Zr that remain fairly constant until 35 cm, whereas Ti, Si and Al begin low and show an increasing trend, peaking at 35 cm (Fig. 4). All elements decrease and then Ti, Si and Al remain stable until ~ 8 cm, whereas Zr increases, peaking at 15 cm. All elements record a sharp decline at 10 cm, before showing increased fluctuations to the top of the record. Ti, Si and Al all decrease at the top, whereas Zr shows a slight increasing trend.

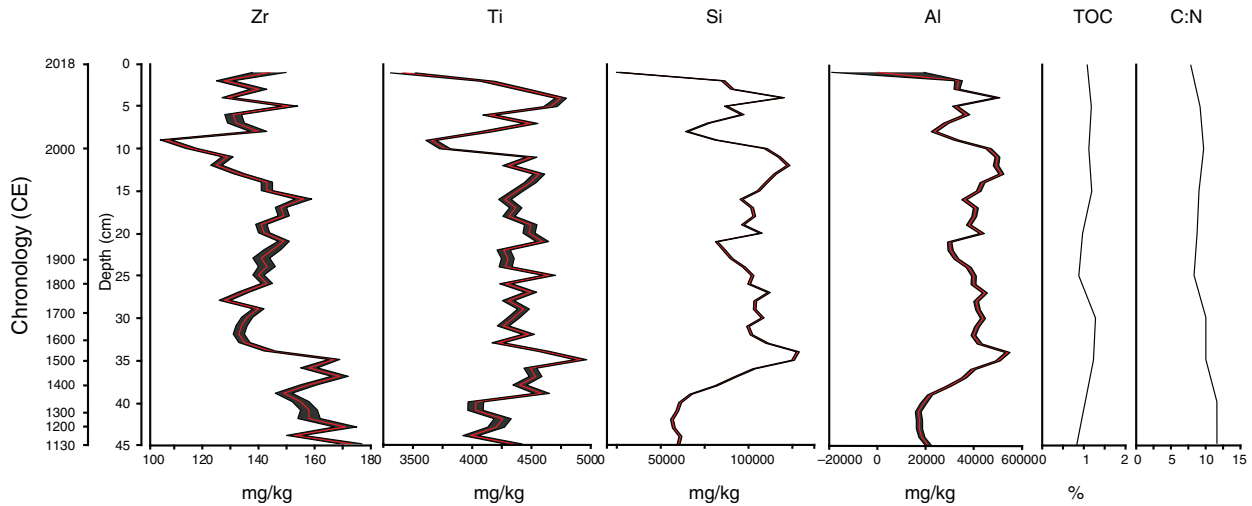


Fig. 4. Tuallka diagram showing XRF elements, total organic carbon and carbon to nitrogen ratio. The red line in the XRF is the recorded element in mg/kg, with the black lines on either side representing the measured error rate.

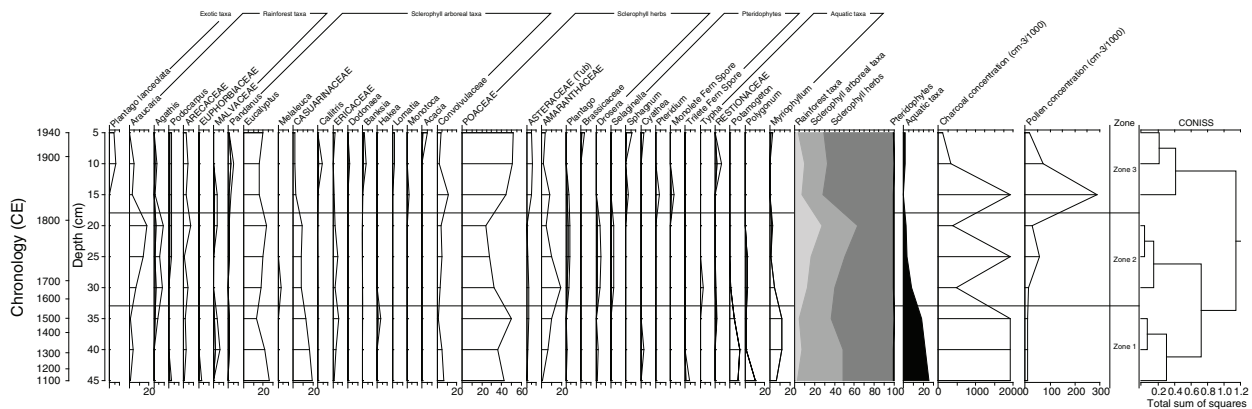


Fig. 5. Lake Mary North pollen diagram including micro-charcoal and pollen concentrations separated into CONISS zones.

Palaeoecology and micro-charcoal

Lake Mary North (LMN1)

Three main biostratigraphic zones were determined using the CONISS analysis (Fig. 5). These are described below.

Zone 1: 46–33 cm; ~1100–1600 CE

Zone 1 shows the greatest representation of aquatic macrophytes (*Potamogeton*, *Polygonum* and *Myriophyllum*) in the record. This zone is dominated by increasing herbaceous taxa (primarily Poaceae) and slightly decreasing sclerophyll arboreal taxa (*Eucalyptus* and Casuarinaceae). Ericaceae peaks at the top of Zone 1. Both pteridophytes and rainforest taxa remain low throughout this zone. Micro-charcoal values record a high concentration (1933200 particles cm^{-3}) for the entire zone.

Zone 2: 32–18 cm; ~1600–1800 CE

There is a shift in dominant vegetation taxa in this zone. Rainforest taxa (particularly *Araucaria* and *Arecaceae*) peak at the top of Zone 2, whereas herbaceous taxa (mostly Poaceae)

decrease. *Eucalyptus*, Casuarinaceae and Ericaceae peak (with the former recording the greatest change) at the top. Aquatics show a decreasing trend, whereas minimal variations occur in pteridophytes. Micro-charcoal values drop to 143300 particles cm^{-3} , before peaking at 25 cm (1933200 particles cm^{-3}). At the top of Zone 2, micro-charcoal concentration declines to 386640 particles cm^{-3} .

Zone 3: 17–5 cm; ~1800–1900 CE

There is an abrupt shift from sclerophyll woodland to savanna conditions (as indicated by the decreased sclerophyll arboreal taxa and the increase in Poaceae and Asteraceae (Tubuliflorae)). Although there is an overall decreasing trend in sclerophyll arboreal taxa (in particular Casuarinaceae), at the top of the record *Eucalyptus* values increase. *Pandanus* peaks during this zone. The exotic species *Plantago lanceolata* appears for the first time. Aquatics completely disappear at the base of this zone, before re-appearing towards the top of the record, with the inclusion of Restionaceae. Rainforest taxa are

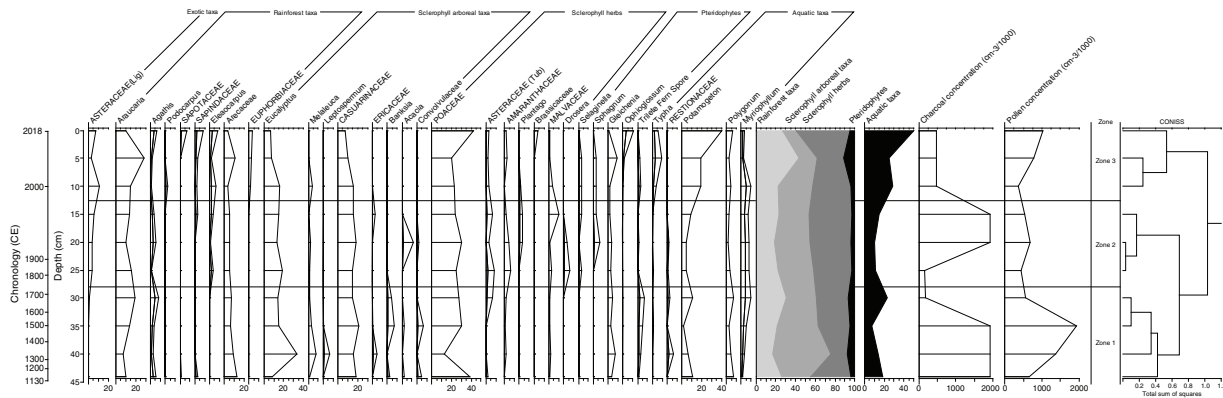


Fig. 6. Tualka pollen diagram including micro-charcoal and pollen concentrations separated into CONISS zones.

present in lower values, whereas pteridophytes show greater variability. Micro-charcoal peaks at the base (1933200 particles cm^{-3}), before decreasing to its lowest concentration throughout the record (113717 particles cm^{-3}).

Tualka (TUA1)

The Tualka pollen results were also broken up into three biostratigraphic zones (Fig. 6).

Zone 1: 45–28 cm; ~1100–1700 CE

There is a shift from more herbaceous (mostly Poaceae) dominated taxa to sclerophyll arboreal taxa (primarily *Eucalyptus*, *Melaleuca* and Casuarinaceae) at the base of this zone. Towards the top of Zone 1, this reverts to greater percentages of herbaceous taxa. Aquatics and rainforest taxa show a decreasing trend, before increasing and peaking at the top of the zone, whereas pteridophytes show two small peaks. Micro-charcoal begins with a high concentration of 1933200 particles cm^{-3} , until 30 cm, where it decreases to its lowest concentration throughout the record (193320 particles cm^{-3}).

Zone 2: 27–13 cm; ~1700–2000 CE

Herbaceous taxa show an increasing trend, with peaks in Asteraceae (Tubuliflorae), Poaceae and Amaranthaceae. Exotic taxa Asteraceae (Liguliflorae) appears in the record at the base of this zone. Aquatic taxa show low percentages, although with an increasing trend. Rainforest taxa slightly decline before increasing to the top of Zone 2. Pteridophyte values are their lowest throughout the record. Micro-charcoal concentration begins low (148707 particles cm^{-3}), before peaking at 20 cm (1933200 particles cm^{-3}) and reaching a plateau for the rest of Zone 2.

Zone 3: 12–0 cm; ~2000–2018 CE

Aquatics peak to their highest percentages at the top of the record (primarily *Potamogeton*). *Typha* peaks during this zone. Both rainforest taxa (namely *Araucaria* and *Arecaceae*) and pteridophytes (*Gleichenia*) peak in the middle of this zone, before decreasing. *Ophioglossum* appears for the first time. Zone 3 shows greater variability in rainforest taxa, and Euphorbiaceae appears for the first time in the record. Sclerophyll arboreal taxa show a decreasing trend to the top of Zone 3,

whereas herbaceous taxa (Poaceae) increase. Micro-charcoal shows decreased values of 843300 particles cm^{-3} , which reach a plateau for the rest of the record.

Discussion

Lake Mary North

The base of the Lake Mary North record shows an infilling of the lake basin. Because Ti, Si and Al all correlate and show similar trends, we are confident that this is presenting a terrigenous sediment input record. Zr shows a greater variance than the other elements; however, it may be that this variance is suggesting a change in particle size (Davies *et al.* 2015). This is correlated with the high ratio of terrigenous sediment, which shows a decreasing trend to ~1700s CE, with TOC values showing the inverse (Fig. 7). With a greater particle size, the TOC concentration will record lower values (Meyers and Teranes 2001). Even though there are increased terrigenous sediment values, the recorded sediment deposited in Lake Mary North is quite low. The C:N ratio at the base of Lake Mary North is in the range of algae (~4–10; Meyers 1994) during the basin infilling. The semi-emergent species *Myriophyllum* and the aquatic taxa *Potamogeton* and *Polygonum* dominate the base of the pollen record as shown in Fig. 7. This suggests that Lake Mary North was a palustrine wetland ~1100 CE, also correlating with variable water depths. Lake Mary North was surrounded by sclerophyll woodland before shifting to a more open grassland-dominated landscape. There is an extended peak in micro-charcoal at the base of this record (~1100 CE), which may be due to increased El Niño–Southern Oscillation (ENSO) activity, which was suggested to be drier and more variable from ~3000 years before present (Barr *et al.* 2019). Variations in the frequency and strength of ENSO can cause increased rate of burning because it enhances both fuel loads with wet years and fire events with dry years (Bradstock 2010; Mooney *et al.* 2011; Barr *et al.* 2019).

Between ~1600 CE and 1800 CE, there is a shift to regionally wetter conditions, which coincides with the Little Ice Age (LIA; ~1450–1850 CE; Rustic *et al.* 2015). During this period, sclerophyll forest dominates the record, with an increasing trend in rainforest taxa (particularly *Araucaria*, *Arecaceae* and *Agathis*) and decreasing sclerophyll herbs, namely grasses (Fig. 7). This correlates with pollen concentrations peaking to

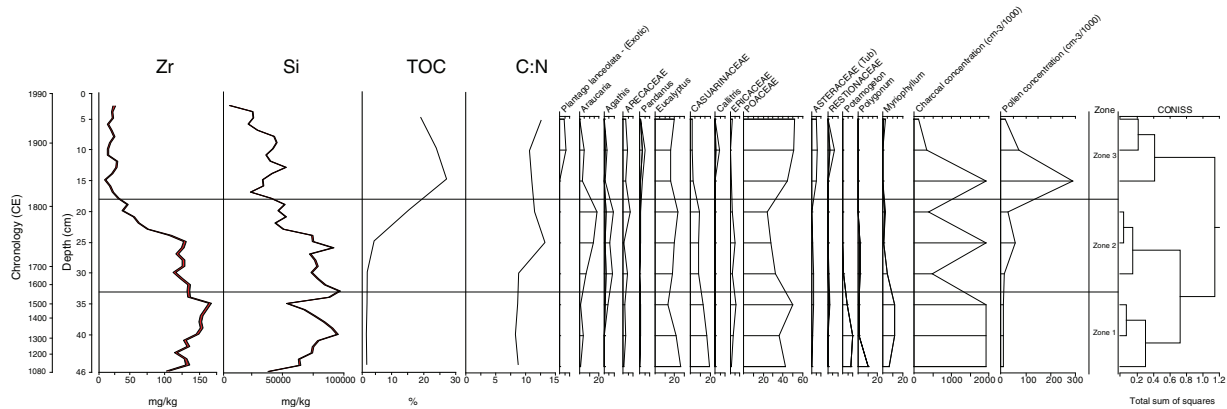


Fig. 7. Lake Mary North summary diagram showing terrigenous input proxies (Zr and Si), total organic carbon (TOC) and carbon to nitrogen (C:N), main pollen taxa and micro-charcoal and pollen concentrations within the CONISS zones.

their highest values in the record, indicating increased vegetation for pollen production and wetter conditions for pollen preservation. C:N values slightly increase, peaking at 15, which indicates an increase in non-algal organic matter (Meyers 1994), perhaps because of the change in surrounding vegetation. Micro-charcoal concentration peaks ~1700 CE, correlating with this regional shift in climate, as does Ericaceae, which suggests landscape disturbance. During these wetter conditions, Lake Mary North records decreased aquatic macrophytes owing to a deeper water column. This corresponds with a shift towards decreasing terrigenous input and increasing TOC trends. In deeper lake basins, where the majority of particles are fine grained, TOC concentrations increase (Meyers and Teranes 2001). This decrease in aquatic macrophytes and shift in the ratio between terrigenous and organic sediment is indicative that Lake Mary North transitioned to lacustrine conditions. Wetter conditions during the LIA in Australia have been recorded in North Stradbroke Island, Queensland (Barr *et al.* 2019), and South Australian lake records (Barr *et al.* 2014), as well as with tree ring data from Tasmania (Cook *et al.* 2000).

There is a major change in vegetation ~1800 CE, which correlates with European occupation and changed land use, starting during the 1840s CE (Seabrook *et al.* 2006). The exotic (introduced) taxa *Plantago lanceolata* appears during this period, providing evidence for human-altered landscape change (Fig. 7). An abrupt increase in grasses then dominate the vegetation record, with low values of sclerophyll arboreal taxa and very little rainforest taxa. Around this time, there was increased disturbance associated with land clearance, as inferred by the greater presence of Asteraceae (Tubuliflorae) (Moss *et al.* 2016), which recorded its highest values at the top of the core. TOC concentration shows a decreasing trend, while C:N continues to show a higher ratio of carbon than nitrogen, indicating a combination of algae and vegetation with a greater carbon content. While Lake Mary North showed a decreasing trend in terrigenous sediment, there is a return to slightly higher values at the top of the record. The sediment deposition at Lake Mary North follows an increasing trend to the top of the record.

During this period, there is a large peak in micro-charcoal, which correlates with a change in fire regimes (Fig. 7). Changes in fire regimes is also indicated by a shift to greater fire-tolerant

Eucalyptus, whereas less fire-resistant species Casuarinaceae is present in very low percentages. This decrease in Casuarinaceae also correlates with European occupation because it was a preferred timber used by early settlers (Crowley and Kershaw 1994). The appearance of *Pandanus* also suggests a fire regime alteration and an opening up of the landscape. Changes in fire regimes are complex and can be due to a variety of factors, such as climate- or human-influenced landscape change. This alteration may be caused by changes in land management practices, from active burning practices associated with Indigenous land management to European fire suppression. This correlates with a shift to very low micro-charcoal concentrations from ~1900 CE to the top of the record. This trend has been recorded in Moss *et al.* (2007, 2011, 2015) and represents a shift to less frequent fire regimes, likely owing to post-European fire suppression.

Aquatics completely disappeared ~1840 CE, before returning ~1890 CE. The reappearance of aquatic macrophytes is likely to indicate a shallowing of Lake Mary North and coincides with El Niño conditions from ~1880 to 1889 CE (Bureau of Meteorology 2021). The shallower conditions of Lake Mary North correlates with the return to palustrine wetland conditions. This coincides with an increase in the C:N ratio, which may be due to the increase in aquatic macrophytes. At this time, there was likely to be a major change in water regime relative to the rest of the record as inferred by the reappearance of semi-emergent species *Myriophyllum*, the first appearance of wetland indicator family Restionaceae (which is commonly found in moist to occasionally waterlogged wetlands) and also the increase in pteridophytes (Fig. 7). Although there have been many historic droughts (1856 CE, 1860 CE, 1878 CE) and floods (1864 CE, 1890 CE, 1893 CE, 1896 CE) between the 1840s CE and ~1890s CE that have affected the Rockhampton area (Bird 1904), the present study does not have a high-enough resolution to record these events and, therefore, shows a general drying up of the wetland.

According to the Queensland Regional Ecosystem classification scheme, just before European occupation, Lake Mary North is characterised as being a coastal/subcoastal freshwater palustrine wetland with permanent or semi-permanent water and aquatic vegetation (RE 8.3.4; Queensland Herbarium 2019; K. Glanville, Queensland Herbarium, pers. comm.). About 1100

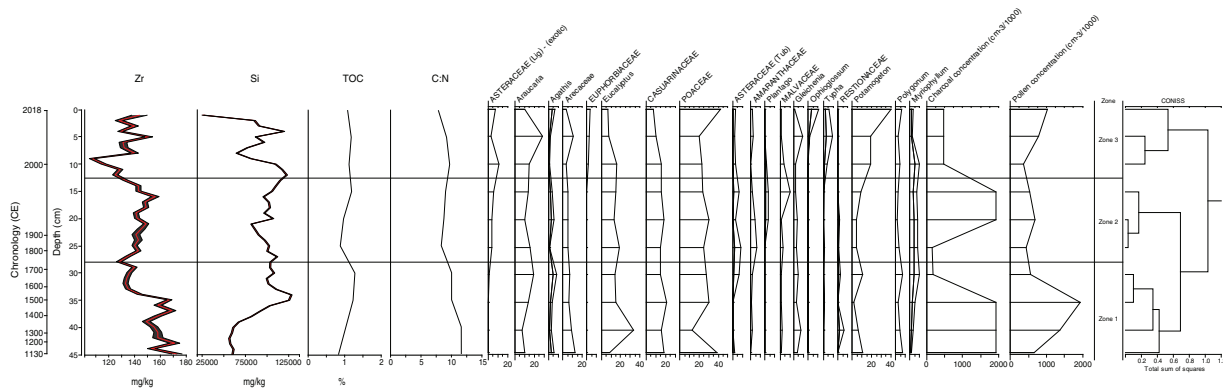


Fig. 8. Tulka summary diagram showing terrigenous input proxies (Zr and Si), total organic carbon (TOC) and carbon to nitrogen (C/N), main pollen taxa and micro-charcoal and pollen concentrations within the CONISS zones.

CE, Lake Mary North was a palustrine wetland surrounded by low to open woodland, dominated by *Eucalyptus*, Casuarinaceae and Poaceae. However, just before European settlement, Lake Mary North recorded regionally wetter conditions, dominated by sclerophyll forest (*Araucaria*, *Agathis*, *Arecaceae*, *Eucalyptus* and Casuarinaceae) with low grass values. Some of this rainforest presence is likely to be due to surrounding microphyll vine forest (RE 11.12.4). Although *Araucaria* pollen can be transported from large distances away (Moss *et al.* 2005), it is more likely that the *Araucaria* pollen came from the nearby outcropping trachytic hills, which are host to notophyll vine forest and vine thickets. Prior to European settlement, Lake Mary North was a lacustrine environment; however, the top of the record suggests a shift to current palustrine conditions. Therefore, this classification of ‘freshwater palustrine conditions’ reflects current and also conditions ~1100 CE; however, this does not correlate with pre-European environmental conditions.

Tulka

The Tulka wetland provides a much more stable hydrological record regarding the presence of constant aquatic taxa. Groundwater-dependent ecosystem (GDE) mapping (Department of Science, Information Technology and Innovation 2015; The State of Queensland 2020) suggests with ‘moderate confidence’ that Tulka might be a GDE, which would explain the constant presence of aquatic macrophytes, even during drier environmental conditions where it superficially appears dry.

Between ~1100 CE and 1300 CE, the Tulka wetland was a shallow lacustrine environment (indicated by the presence of semi-emergent species *Myriophyllum*) surrounded by a mix of sclerophyll woodland and forest, before changing primarily to sclerophyll woodland ~1500 CE (Fig. 8). It is likely that Tulka was fringed by *Eucalyptus* ~1300 CE (owing to the high *Eucalyptus* percentage). This change in vegetation coincides with Zr recording increased values, and Si, Ti and Al showing the opposite. It is inferred that there is a shift from coarser particles to finer, which may indicate changes in sediment transport owing to changing surrounding vegetation. C:N values remain ~11, which suggests a combination of algae and vegetation with greater carbon content during this period. TOC values are minimal, with little change throughout this

record; however, there is a slight increasing trend. Low TOC may indicate that Tulka was experiencing seasonally/annually drier conditions and, therefore, not preserving organic matter. This was a period of climatic variability (as indicated by high micro-charcoal concentrations), which was similarly recorded at Lake Mary and is likely to represent increased ENSO variability. This increased micro-charcoal concentration may be due to higher fuel loads associated with a greater tree cover.

Tulka records regionally wetter conditions during the LIA, with a greater regional presence of arboreal taxa (as shown by the increased rainforest taxa and consistent sclerophyll arboreal taxa in Fig. 8). This is correlated with the large concentration of preserved pollen, which indicates conditions conducive to preservation (i.e. anaerobic, thus reflecting regular water cover in Tulka). There is a marked increase in finer particles (increased Si, Al and Ti), indicating a deeper water column. TOC slightly peaks, whereas C:N marginally decreases.

Micro-charcoal concentrations decrease to their lowest values in the record pre-European settlement, and pollen concentration also decreases (Fig. 8). It may be that this is recording drier conditions (e.g. an extreme El Niño event ~1650s CE; Liu *et al.* 2017); however, a higher resolution record is required to further investigate climate variability and how wetlands in the NACC react during the LIA. Tulka records drier conditions after the LIA, which is shown by the peaks in Asteraceae (Tubuliflorae), Poaceae, Amaranthaceae, increasing trend in Malvaceae and a decrease in rainforest taxa. Tibby *et al.* (2018) also suggested a post-LIA dry period in eastern Australia. Asteraceae (Liguliflorae) appears around the 1840s CE, which coincides with European occupation. Both *Eucalyptus* and grasses peak, likely as a result of European land-use practices. Changes in land use are further indicated by the peak in micro-charcoal in the ~1900s CE, representing a probable shift in fire regimes from the cessation of indigenous burning, causing a high fuel load that increased fire intensities (Moss *et al.* 2016). The Tulka wetland appears fairly stable during this period, with minimal changes in aquatic macrophytes and terrigenous sediment. From the ~1900s CE to present, there appears to be an increase in sediment entering Tulka.

Towards the top of the core, aquatic taxa (namely *Potamogeton*) rapidly increase to ~50%. *Potamogeton* grows

in eutrophic conditions and, therefore, the larger representation in the pollen record may be a combination of drier conditions causing a shallowing of the lake and cattle contributing to nutrients in the soil (Leoni *et al.* 2016). This correlates with decreased micro-charcoal because there was less fuel to ignite. This may also represent post-European fire suppression regimes. Further evidence of human landscape alteration is the appearance of Euphorbiaceae (*Ricinus communis*, commonly known as castor oil plant), an introduced species widespread in riparian habitats within the region (Business Queensland 2020).

At the top of the record, rainforest taxa record a higher representation than do sclerophyll arboreal taxa. It is likely that the pollen record is showing a reduced extent of sclerophyllous woodland, rather than an increase in rainforest-dominated landscape. This was further corroborated by examination of past satellite imagery and aerial photographs, which showed a decreased amount of woodland post-1950s CE (State of Queensland 1952; Google Earth 2006; DigitalGlobe 2012). Grasses show their highest values to present. Coarser terrigenous sediment shows a dip at 10 cm, whereas finer grains peak before both coarse and fine sediments increase and show more fluctuations to the top of the core. This may be attributed to a combination of historical land clearing and drought causing more exposed soil (e.g. the Millennium Drought; 2001–2009 CE; van Dijk *et al.* 2013), which affected Tualka, causing more sediment instability and runoff.

According to the RE 11.3.27g description, before European settlement, Tualka was, and currently is, a freshwater floodplain lake that may have fringing *Eucalyptus coolabah* woodland and sedgeland (Queensland Herbarium 2019). Surrounding Tualka, the vegetation would have been shrubby woodland dominated by *Eucalyptus populnea* and *Eremophila mitchelli* (RE 11.9.7; Queensland Herbarium 2019). The Tualka record indicates that this lacustrine environment has been relatively stable since ~1130 CE, with sclerophyll woodland and forest in the surrounding landscape, and therefore follows the RE classification. Tualka has a consistent presence of rainforest taxa (*Araucaria* and *Arecaceae*) throughout the record, peaking both during the LIA and at the top of the core. The presence of *Arecaceae* (possibly the Dawson River fan palm *Livistona nitida*) is most likely to be due to wetter refugia areas situated along the upper Dawson River and also possibly from Isla Gorge, Nathan Gorge or Carnarvon Gorge, and the *Araucaria* is once again likely to be located further away. Although regionally wetter conditions are recorded pre-European settlement, locally vegetation does not seem to shift greatly. However, drier conditions do appear to dominate after European occupation. There is a clear shallowing trend towards the top of the record, with the increase in aquatic taxa *Potamogeton* and *Typha*. This correlates with changes in sediment patterns ~1900s CE, where a trend in greater sediment accumulation occurs.

Wetland comparison

Whereas Tualka recorded a lacustrine environment for the past ~1000 years, Lake Mary North showed palustrine conditions from ~1100 CE to present, except between ~1500 CE and ~1900 CE, when it shifted to a lacustrine environment. Climatic variability was recorded from both sites between ~1100 CE and ~1500 CE (as determined by high micro-charcoal

concentration). During this period, both wetlands also recorded woodland/savanna surroundings around shallow waterbodies.

Both wetlands recorded regionally wetter conditions during the LIA, with increased water. Lake Mary North shifted to a more lacustrine environment, whereas Tualka recorded deeper water conditions. A low micro-charcoal concentration ~1600 CE is consistent across both wetlands; however, micro-charcoal concentration in Tualka remained low until ~1800 CE, whereas it peaked at Lake Mary North at ~1700 CE. This age variation in micro-charcoal peaks is likely to reflect different fire regimes owing to local site conditions (Moss *et al.* 2013).

Both Lake Mary North and Tualka recorded the presence of exotic taxa ~1840 CE (*Plantago lanceolata* and *Asteraceae* (Liguliflorae) respectively). This period was dominated by drier conditions and increased land disturbance, as shown by increased *Asteraceae* (Tubuliflorae) and peaks in *Amaranthaceae* in both records, as well as the return to palustrine conditions at Lake Mary North. Both wetlands recorded increased grasses, owing to changed land management associated with pastoralism. Lake Mary North showed decreased values in sclerophyll arboreal taxa, whereas Tualka appeared relatively unaltered. Lake Mary North recorded a peak in micro-charcoal ~1840 CE, before it dropped to its lowest values at the top of the record. Tualka also recorded a micro-charcoal peak during the ~1900s CE, before following the same trend as Lake Mary North. These peaks represent a shift in fire regimes to infrequent burning from European fire suppression. At the top of the Tualka record, there is a shift from sclerophyll woodland to savanna conditions, as shown by the peak in herbaceous taxa and a decrease in arboreal taxa. Tualka also recorded increased aquatic macrophytes and pteridophytes towards the top of the core, indicating a shallowing of the lake.

Both wetlands show a diverse site history affected by climatic variability and human landscape alteration. At the top of the Lake Mary North record, increased presence of landscape alteration was determined, whereas Tualka indicated a more stable record, with some evidence of decreased arboreal taxa and increased shallowing of the lake. Both sites indicate changes in sedimentation patterns, with more sediment being deposited at Lake Mary North from the ~1700s CE and later at Tualka (~1900s CE). Increased sediment deposition post-European settlement has also been recorded in floodplain wetlands within the Burdekin Catchment, NACC (Tibby *et al.* 2019).

Conclusions

This research has shown that the Regional Ecosystem classification is broadly applicable for monitoring purposes, but it is unable to account for fluctuating aquatic vegetation baselines associated with variable climate conditions and hydrological regimes over longer time periods. This study also suggests changes in catchment conditions and the need for further investigation of sedimentation rates and processes potentially affecting these wetlands. Diatom analysis could help provide information on past and present water quality, such as changes in salinity or nutrient availability, and therefore complement our interpretations regarding relative changes in water depth and also increased nutrients determined by the pollen record. The inclusion of younger dating methods and plant macrofossil analysis to these sites would provide more insight into modern

ecological factors affecting the wetlands and also present a greater understanding of local vegetation. Whereas the results of this study are informative at the individual wetland scale, aggregation-level studies are needed for NACC-wide management and restoration decision-making. Specifically, further research is needed to determine the degree to which the individual findings for Lake Mary North and Tualka are representative of other wetlands within the Hedlow Creek and the Palm Tree Robinson Creek aggregations and those aggregations overall.

Data availability statement

The raw data from this research are available on request to the corresponding author.

Conflicts of interest

The authors on this paper declare that they have no conflicts of interest.

Declaration of funding

This project was funded by the Queensland Government and undertaken as part of the Great Barrier Reef Catchments Wetland Condition Monitoring program with in-kind contributions from The University of Queensland.

Acknowledgements

We thank Terri Sutcliffe from the EcoSciences Precinct for all her help with the site image. Johanna Hanson also thanks Dr Philip Stewart for his help with rbacon.

References

- Australian Government and Queensland Government (2016). Wetland condition methods: Great Barrier Reef Report Card 2016, Reef Water Quality Protection Plan. Available at https://www.reefplan.qld.gov.au/_data/assets/pdf_file/0024/46167/report-card-2016-wetland-condition-methods.pdf [Verified 15 June 2021]
- Australian Government: Great Barrier Reef Marine Park Authority (2001). Population and Major Land Use in the Great Barrier Reef Catchment Area: Spatial and Temporal Trends. Available at <https://elibrary.gbrmpa.gov.au/jspui/retrieve/0e97ac61-a021-4e1f-83d1-e5db5d465165/Population-and-major-land-use-in-the-Great-Barrier-Reef-catchment-area-spatial-and-temporal-trends.pdf> [Verified 14 June 2021]
- Barr, C., Tibby, J., Gell, P., Tyler, J., Zawadzki, A., and Jacobsen, G. E. (2014). Climate variability in south-eastern Australia over the last 1500 years inferred from the high-resolution diatom records of two crater lakes. *Quaternary Science Reviews* **95**, 115–131. doi:10.1016/J.QUASCIREV.2014.05.001
- Barr, C., Tibby, J., Leng, M. J., Tyler, J. J., Henderson, A. C. G., Overpeck, J. T., Simpson, G. L., Cole, J. E., Phipps, S. J., Marshall, J. C., McGregor, G. B., Hua, Q., and McRobie, F. H. (2019). Holocene El Niño–Southern Oscillation variability reflected in subtropical Australian precipitation. *Scientific Reports* **9**, 1627. doi:10.1038/S41598-019-38626-3
- Bird, J. T. S. (1904). The early history of Rockhampton, dealing chiefly with events up till 1870. The Morning Bulletin Office, Kast Street, Rockhampton, Qld, Australia.
- Blaauw, M., and Christen, A. (2011). Flexible paleoclimate age-depth models using an autoregressive gamma process. *Bayesian Analysis* **6**(3), 457–474. doi:10.1214/BA/1339616472
- Bradstock, R. A. (2010). A biogeographic model of fire regimes in Australia: current and future implications. *Global Ecology and Biogeography* **19**, 145–158. doi:10.1111/J.1466-8238.2009.00512.X
- Bronk Ramsey, C. (1995). Radiocarbon calibration and analysis of stratigraphy: the OxCal program. *Radiocarbon* **37**(2), 425–430.
- Bronk Ramsey, C. (2008). Deposition models for chronological records. *Quaternary Science Reviews* **27**, 42–60. doi:10.1016/J.QUASCIREV.2007.01.019
- Bronk Ramsey, C. (2009). Bayesian analysis of radiocarbon dates. *Radiocarbon* **51**(1), 337–360. doi:10.1017/S003822200033865
- Bureau of Meteorology (2006). Climate classification maps. Commonwealth of Australia. Available at http://www.bom.gov.au/jsp/ncc/climate_averages/climate-classifications/index.jsp
- Bureau of Meteorology (2021). Southern Oscillation Index (SOI) since 1876. Available at <http://www.bom.gov.au/climate/enso/soi/> [Verified 15 February 2021]
- Business Queensland (2020). Castor oil plant. Queensland Government, Australia. Available at <https://www.business.qld.gov.au/industries/farms-fishing-forestry/agriculture/land-management/health-pests-weeds-diseases/weeds-diseases/invasive-plants/other/castor-oil-bush> [Verified 13 January 2021]
- Commonwealth of Australia (2015). Reef 2050 Long-term Sustainability Plan. Available at <https://www.environment.gov.au/system/files/resources/d98b3e53-146b-4b9c-a84a-2a22454b9a83/files/reef-2050-long-term-sustainability-plan.pdf> [Verified 14 June 2021]
- Cook, E. R., Buckley, B. M., D'Arrigo, R. D., and Peterson, M. J. (2000). Warm-season temperatures since 1600 BC reconstructed from Tasmanian tree rings and their relationship to large-scale sea surface temperature anomalies. *Climate Dynamics* **16**, 79–91. doi:10.1007/S003820050006
- Crowley, G. M., and Kershaw, P. (1994). Late Quaternary environmental change and human impact around Lake Bolac, western Victoria, Australia. *Journal of Quaternary Science* **9**(4), 367–377. doi:10.1002/JQS.3390090407
- Davies, S. J., Lamb, H. F., and Roberts, S. J. (2015). Micro-XRF core scanning in palaeolimnology: recent developments. In 'Micro-XRF Studies of Sediment Cores: Applications of a Non-destructive Tool for the Environmental Sciences'. (Eds I. W. Croudace and R. G. Rothwell.) pp. 189–226. (Springer: Dordrecht, Netherlands.)
- Department of Agriculture, Water and the Environment (n.d.). Directory of Important Wetlands in Australia, Australian Government. Available at <https://www.environment.gov.au/water/wetlands/australian-wetlands-database/directory-important-wetlands> [Verified 15 June 2021]
- Department of Environment and Science Queensland (2019). Wetland mapping background, Wetland Info website. Available at <https://wetlandinfo.des.qld.gov.au/wetlands/facts-maps/wetland-background/> [Verified 24 September 2020]
- Department of Science, Information Technology and Innovation (2015). Groundwater Dependent Ecosystem Mapping Report: Comet, Dawson and Mackenzie River drainage sub-basins. The State of Queensland. Available at <https://www.publications.qld.gov.au/dataset/groundwater-dependent-ecosystem-mapping-report-v1-0/resource/9b52a6c5-3461-47ef-b3a0-5aa3d5d38cf4>
- DigitalGlobe (2012). Tualka 25°13'6.79"S, 149°42'0.63"E, Maxar Technologies Inc., CO, USA. Available at <https://discover.digitalglobe.com/>.
- Dudgeon, D., Arthington, A. H., Gessner, M. O., Kawabata, Z. I., Knowler, D. J., Lévêque, C., Naiman, R. J., Prieur-Richard, A. H., Soto, D., Stiassny, M. L. J., and Sullivan, C. A. (2006). 'Freshwater biodiversity: Importance, threats, status and conservation challenges. *Biological Reviews of the Cambridge Philosophical Society* **81**, 163–182. doi:10.1017/S1464793105006950
- Evans, G., Augustinus, P., Gadd, P., Zawadzki, A., and Ditchfield, A. (2019). A multi-proxy μ -XRF inferred lake sediment record of environmental change spanning the last ca. 2230 years from Lake Kanono, Northland, New Zealand. *Quaternary Science Reviews* **225**, 106000. doi:10.1016/J.QUASCIREV.2019.106000

- Finlayson, C. M., and Rea, N. (1999). Reasons for the loss and degradation of Australian wetlands. *Wetlands Ecology and Management* **7**, 1–11. doi:10.1023/A:1008495619951
- Finlayson, C. M., Capon, S. J., Rissik, D., Pittock, J., Fisk, G., Davidson, N. C., Bodmin, K. A., Papas, P., Robertson, H. A., Schallenberg, M., Saintilan, N., Edyvane, K., and Bino, G. (2017). Policy considerations for managing wetlands under a changing climate. *Marine and Freshwater Research* **68**, 1803–1815. doi:10.1071/MF16244
- Gangloff, M. M., Edgar, G. J., and Wilson, B. (2016). Imperilled species in aquatic ecosystems: emerging threats, management and future prognoses. *Aquatic Conservation* **26**, 858–871. doi:10.1002/AQC.2707
- Gell, P., and Reid, M. (2014). Assessing change in floodplain wetland condition in the Murray–Darling Basin, Australia. *Anthropocene* **8**, 39–45. doi:10.1016/J.ANCENE.2014.12.002
- Gell, P., Fluin, J., Tibby, J., Hancock, G., Harrison, J., Zawadzki, A., Haynes, D., Khanum, S., Little, F., and Walsh, B. (2009). Anthropogenic acceleration of sediment accretion in lowland floodplain wetlands, Murray–Darling Basin, Australia. *Geomorphology* **108**(1–2), 122–126. doi:10.1016/J.GEOMORPH.2007.12.020
- Gell, P., Finlayson, C. M., and Davidson, N. C. (2016). Understanding change in the ecological character of Ramsar wetlands: perspectives from a deeper time – synthesis. *Marine and Freshwater Research* **67**, 869–879. doi:10.1071/MF16075
- Gilbert, M. (2000). Population and major land use in the Great Barrier Reef catchment are: spatial and temporal trends. GBRMPA Research Publication Series, Great Barrier Reef Marine Park Authority, Townsville, Qld, Australia.
- Google Earth (2006). Google Earth v. 7.3.3.7786. Tualka 25°13'6.79''S, 149°42'0.63''E. Available at <https://earth.google.com/web/search/+25%2c2%b013%276.79%22S,+149%2c2%b042%270.63%22E%27/@-25.20466316,149.68558546,249.33783969a,23087.40623504d,35y,-162.23675503h,45.14078735t,0r/=CmIaOBlyGQBzIBPzNznAIULPZtVntmJAKh4gMjXCSDzEzYuNzkiUywgMTQ5wrA0MicwLjYzlkUYAiABliYKJAIQ9YWjS3YwwBFMDnZdJ3owwBmuLq-W9PdiwCExyRhPhiwA> [Verified 30 November 2006]
- Grimm, E. C. (1987). CONISS: a FORTRAN 77 program for stratigraphically constrained cluster analysis by the method of incremental sum of squares. *Computers & Geosciences* **13**, 13–35. doi:10.1016/0098-3004(87)90022-7
- Habermehl, M. A., and Lau, J. E. (1997). Hydrology of the Great Artesian Basin, Australia, map at scale 1:2 500 000. Australian Geological Survey Organisation, Canberra, ACT, Australia.
- Hogg, A., Heaton, T., Hua, Q., Palmer, J., Turney, C., Southon, J., Bayliss, A., Blackwell, P., Boswijk, G., Bronk Ramsey, C., Petchey, F., Reimer, R., and Wacker, L. (2020). SHCal20 Southern Hemisphere calibration, 0–55 000 years cal BP. *Radiocarbon* **62**, 759–778. doi:10.1017/RDC.2020.59
- Hua, Q., Barbetti, M., and Rakowski, A. J. (2013). Atmospheric Radiocarbon for the Period 1950–2010. *Radiocarbon* **55**(4), 2059–2072. doi:10.2458/AZU_JS_RC.V55I2.16177
- Kershaw, A. P. (1997). A modification of the Troels-Smith system of sediment description and portrayal. *Quaternary Australasia* **15**, 63–68.
- Köppen, W. (1931). 'Klimakarte der Erde.' (Grundriss der Klimakunde: Berlin and Leipzig.)
- Kylander, M. E., Ampel, L., Wohlfarth, B., and Veres, D. (2011). High-resolution X-ray fluorescence core scanning analysis of Les Echets (France) sedimentary sequence: new insights from chemical proxies. *Journal of Quaternary Science* **26**, 109–117. doi:10.1002/JQS.1438
- Leoni, B., Marti, C. L., Forasacco, E., Mattavelli, M., Soler, V., Fumagalli, P., Imberger, J., Rezzonico, S., and Garibaldi, L. (2016). The contribution of *Potamogeton crispus* to the phosphorus budget of an urban shallow lake: Lake Monger, Western Australia. *Limnology* **17**(2), 175–182. doi:10.1007/S10201-015-0465-4
- Lewis, S. E., Bartley, R., Wilkinson, S. N., Bainbridge, Z. T., Henderson, A. E., James, C. S., Irvine, S. A., and Brodie, J. E. (2021). Land use change in the river basins of the Great Barrier Reef, 1860 to 2019: a foundation for understanding environmental history across the catchment to reef continuum. *Marine Pollution Bulletin* **166**, 112193. doi:10.1016/J.MARPOLBUL.2021.112193
- Liu, Y., Cobb, K. M., Song, H., Li, Q., Li, Y.-Y., Nakatsuka, T., An, Z., Zhou, W., Cai, Q., Li, J., Leavitt, S. W., Sun, C., Mei, R., Shen, C.-C., Chan, M.-H., Sun, J., Yan, L., Lei, Y., Ma, Y., Li, X., Chen, D., and Linderholm, H. W. (2017). Recent enhancement of central Pacific El Niño variability relative to last eight centuries. *Nature Communications* **8**, 15386. doi:10.1038/NCOMMS15386
- Longman, J., Veres, D., and Wennrich, V. (2019). Utilisation of XRF core scanning on peat and other highly organic sediments. *Quaternary International* **514**, 85–96. doi:10.1016/J.QUAINT.2018.10.015
- Meyers, P. A. (1994). Preservation of elemental and isotopic source identification of sedimentary organic matter. *Chemical Geology* **114**, 289–302. doi:10.1016/0009-2541(94)90059-0
- Meyers, P. A., and Teranes, J. L. (2001). Sediment organic matter. In 'Tracking environmental change using lake sediments: physical and geochemical methods'. (Eds W. M. Last and J. P. Smol.) pp. 239–269. (Kluwer Academic Publishers: Dordrecht, Netherlands.)
- Mooney, S. D., Harrison, S. P., Bartlein, P. J., Danianu, A. L., Stevenson, J., Brownlie, K. C., Buckman, S., Cupper, M., Hope, J., Kershaw, P., Kenyon, C., McKenzie, M., and Williams, N. (2011). Late Quaternary fire regimes of Australasia. *Quaternary Science Reviews* **30**, 28–46. doi:10.1016/J.QUASCIREV.2010.10.010
- Moss, P. T. (2013). Palynology and its application to geomorphology. In 'Treatise on Geomorphology, vol. 14'. (Eds J. F. Shroder, A. D. Switzer and D. M. Kennedy.) pp. 315–325. (Academic Press: San Diego, CA, USA.)
- Moss, P. T., Kershaw, P. A., and Grindrod, J. (2005). Pollen transport and deposition in riverine and marine environments within the humid tropics of northeastern Australia. *Review of Palaeobotany and Palynology* **134**, 55–69. doi:10.1016/J.REVPALBO.2004.11.003
- Moss, P. T., Thomas, I., and Macphail, M. (2007). Late Holocene vegetation and environments of the Mersey Valley, Tasmania. *Australian Journal of Botany* **55**, 74–82. doi:10.1071/BT06010
- Moss, P. T., Petherick, L., and Neil, D. (2011). Environmental change at Myora Springs, North Stradbroke Island over the last millennium. *Proceedings of the Royal Society of Queensland* **117**, 133–140.
- Moss, P. T., Tibby, J., Petherick, L., McGowan, H., and Barr, C. (2013). Late Quaternary vegetation history of North Stradbroke Island, Queensland, eastern Australia. *Quaternary Science Reviews* **74**, 257–272. doi:10.1016/J.QUASCIREV.2013.02.019
- Moss, P., Mackenzie, L., Ulm, S., Sloss, C., Rosendahl, D., Petherick, L., Steinberger, L., Wallis, L., Heijns, H., Petchey, F., and Jacobsen, G. (2015). Environmental context for late Holocene human occupation of the South Wellesley Archipelago, Gulf of Carpentaria, northern Australia. *Quaternary International* **385**, 136–144. doi:10.1016/J.QUAINT.2015.02.051
- Moss, P. T., Gehrels, R. W., and Callard, S. L. (2016). European impacts on coastal eastern Tasmania: insight from a high-resolution palynological analysis of a salt-marsh core. *Frontiers in Ecology and Evolution* **4**(105). doi:10.3389/FEVO.2016.00105
- Neldner, V. J., Butler, D. W., and Guymer, G. P. (2019). Queensland's regional ecosystems: building and maintaining a biodiversity inventory, planning framework and information system for Queensland, Version 2.0. Queensland Herbarium, Queensland Department of Environment and Science, Brisbane, Qld, Australia.
- Ogden, R. W. (2000). Modern and historical variation in aquatic macrophyte cover of billabongs associated with catchment development. *Regulated Rivers* **16**, 497–512. doi:10.1002/1099-1646(200009/10)16:5<497::AID-RRR600>3.0.CO;2-Y
- Olsen, J., Björck, S., Leng, M. J., Gudmundsdóttir, E. R., Odgaard, B. V., Lutz, C. M., Kendrick, C. P., Andersen, T. J., and Seidenkrantz, M.

- (2010). Lacustrine evidence of Holocene environmental change from three Faroes lakes: a multiproxy XRF and stable isotope study. *Quaternary Science Reviews* **29**, 2764–2780. doi:10.1016/J.QUASCIREV.2010.06.029
- Pasut, C., Tang, F. H. M., Hamilton, D. P., and Maggi, F. (2021). Carbon, nitrogen, sulfur elemental fluxes in the soil and exchanges with the atmosphere in Australian tropical, temperate, and arid wetlands. *Atmosphere* **12**, 42. doi:10.3390/ATMOS12010042
- Queensland Government (2014). Regional ecosystem framework. Available at <https://www.qld.gov.au/environment/plants-animals/plants/ecosystems/descriptions/framework>. [Verified 11 November 2020]
- Queensland Herbarium (2019). Regional Ecosystem Description Database (REDD), version 11.1. Available at <https://www.qld.gov.au/environment/plants-animals/plants/ecosystems/descriptions/download> [Verified 11 November 2020]
- Reid, A. J., Carlson, A. K., Creed, I. F., Eliason, E. J., Gell, P. A., Johnson, P. T. J., Kidd, K. A., MacCormack, T. J., Olden, J. D., Ormerod, S. J., Dudgeon, D., and Cooke, S. J. (2019). Emerging threats and persistent conservation challenges for freshwater biodiversity. *Biological Reviews of the Cambridge Philosophical Society* **94**, 849–873. doi:10.1111/BRV.12480
- Rustic, G. T., Koutavas, A., Marchitto, T. M., and Linsley, B. K. (2015). Dynamical excitation of the tropical Pacific Ocean and ENSO variability by Little Ice Age cooling. *Science* **350**, 1537–1541. doi:10.1126/SCIENCE.AAC9937
- Schneider, C., Flörke, M., De Stefano, L., and Petersen-Perlman, J. D. (2017). Hydrological threats to riparian wetlands of international importance – a global quantitative and qualitative analysis. *Hydrology and Earth System Sciences* **21**, 2799–2815. doi:10.5194/HESS-21-2799-2017
- Seabrook, L., McAlpine, C. M., and Fensham, R. (2006). Cattle, crops and clearing: regional drivers of landscape change in the Brigalow Belt, Queensland, Australia, 1840–2004. *Landscape and Urban Planning* **78**, 373–385. doi:10.1016/J.LANDURBPLAN.2005.11.007
- State of Queensland (1952). Queensland Aerial Photography Program (Ghinghinda 1952), Scale: 1: 24 000, Film No. QAP269, Frame No. 54.
- State of Queensland (2018). Reef 2050 Water Quality Improvement Plan 2017–2022, Report 31359. Available at https://www.reefplan.qld.gov.au/__data/assets/pdf_file/0017/46115/reef-2050-water-quality-improvement-plan-2017-22.pdf [Verified 11 November 2020]
- The State of Queensland (2020). Wetland maps. Available at <https://wetlandinfo.des.qld.gov.au/wetlandmaps/> [Verified 14 January 2021]
- Tibby, J., Tyler, J. J., and Barr, C. (2018). Post little ice age drying of eastern Australia conflates understanding of early settlement impacts. *Quaternary Science Reviews* **202**, 45–52. doi:10.1016/J.QUASCIREV.2018.10.033
- Tibby, J., Barr, C., Marshall, J. C., Richards, J., Perna, C., Fluin, J., and Cadd, H. R. (2019). Assessing the relative impacts of land-use change and river regulation on Burdekin River (Australia) floodplain wetlands. *Aquatic Conservation* **29**, 1712–1725. doi:10.1002/AQC.3151
- Tjallingii, R., Röhl, U., Kölling, M., and Bickert, T. (2007). Influence of the water contents on X-ray fluorescence core scanning measurements in soft marine sediments. *Geochemistry Geophysics Geosystems* **8**, Q02004. doi:10.1029/2006GC001393
- Troels-Smith, J. (1955). Characterisation of unconsolidated sediments. *Danmarks Geologiske Undersøgelse, series IV* **3**(10), 73.
- van der Kaars, C. (1991). Palynology of eastern Indonesian marine piston-cores: a Late Quaternary vegetational and climatic record from Australia. *Palaeogeography, Palaeoclimatology, Palaeoecology* **85**, 239–302. doi:10.1016/0031-0182(91)90163-L
- van Dijk, A. I. J. M., Beck, H. E., Crosbie, R. S., de Jeu, R. A. M., Liu, Y. Y., Podger, G. M., Timbal, B., and Viney, N. R. (2013). The Millennium Drought in southeast Australia (2001–2009): natural and human causes and implications for water resources, ecosystems, economy, and society. *Water Resources Research* **49**, 1040–1057. doi:10.1002/WRCR.20123
- Walsh, G. L. (1999). ‘Canarvon and beyond.’ (Takaraka Nowan Kas Publications: Canarvon Gorge, Qld, Australia.)
- Walter, F., and Willy, T. (2004). Concentration estimates in pollen slides: accuracy and potential errors. *The Holocene* **15**(2), 293–297.
- Wang, X., van der Kaars, S., Kershaw, A. P., Bird, M., and Jansen, F. (1999). A record of fire, vegetation and climate through the last three glacial cycles from Lombok Ridge core G6-4, eastern Indian Ocean, Indonesia. *Palaeogeography, Palaeoclimatology, Palaeoecology* **147**, 241–256. doi:10.1016/S0031-0182(98)00169-2
- Waterhouse, J., Henry, N., Mitchell, C., Smith, R., Thomson, B., Carruthers, C., Bennett, J., Brodie, J., McCosker, K., Norhey, A., Poggio, M., Moravek, T., Gordon, B., Orr, G., Silburn, M., Shaw, M., Bickle, M., Ronan, M., Turner, R., Waters, D., Tindall, D., Trevithick, R., Ryan, T., VanderGragt, M., Houlden, B., and Robillot, C. (2018). Paddock to Reef Integrated Monitoring, Modelling and Reporting Program; Program design 2018–2022, Australian Government and Queensland Government. Available at https://www.reefplan.qld.gov.au/__data/assets/pdf_file/0026/47249/paddock-to-reef-program-design.pdf [Verified 14 June 2021]
- Willmott, W. F., O’Flynn, M. L., and Trezise, D. L. (1986). Rockhampton Region, Queensland, 1:100 000 geological map commentary. Sheets 8951 & 9051. Geological Survey of Queensland 1v. Geoscience Australia. Australian Government.
- Wingard, G. L., Bernhardt, C. E., and Wachnicka, A. H. (2017). The role of palaeoecology in restoration and resource management- the past as a guide to future decision-making: review and example from the Greater Everglades ecosystem, U.S.A. *Frontiers in Ecology and Evolution* **5**, 11.

Handling Editor: Colin Finlayson